MECHANISMS OF DEVELOPMENT 136 (2015) 99–110

Available at www.sciencedirect.com

ScienceDirect

journal homepage: www.elsevier.com/locate/modo

Normal table of embryonic development in the four-toed salamander, *Hemidactylium scutatum*

C.A. Hurney [a,*], S.K. Babcock [a], D.R. Shook [b], T.M. Pelletier [a], S.D. Turner [c], J. Maturo [a], S. Cogbill [a], M.C. Snow [a], K. Kinch [a]

[a] Department of Biology, MSC 7801, James Madison University, Harrisonburg, VA 22807
[b] Department of Biology, P.O. Box 400328, University of Virginia, Charlottesville, VA 22904
[c] Department of Public Health Sciences, University of Virginia School of Medicine, Charlottesville, Virginia 22908

ARTICLE INFO

Article history:
Received 17 September 2014
Received in revised form
30 November 2014
Accepted 31 December 2014
Available online 21 January 2015

Keywords:
Embryonic development
Plethodontid
Normal table
Amphibian

ABSTRACT

We present a complete staging table of normal development for the lungless salamander, *Hemidactylium scutatum* (Caudata: Plethodontidae). Terrestrial egg clutches from naturally ovipositing females were collected and maintained at 15 °C in the laboratory. Observations, photographs, and time-lapse movies of embryos were taken throughout the 45-day embryonic period. The complete normal table of development for *H. scutatum* is divided into 28 stages and extends previous analyses of *H. scutatum* embryonic development (Bishop, 1920; Humphrey, 1928). Early embryonic stage classifications through neurulation reflect criteria described for *Xenopus laevis*, *Ambystoma maculatum* and other salamanders. Later embryonic stage assignments are based on unique features of *H. scutatum* embryos. Additionally, we provide morphological analysis of gastrulation and neurulation, as well as details on external aspects of eye, gill, limb, pigmentation, and tail development to support future research related to phylogeny, comparative embryology, and molecular mechanisms of development.

1. Introduction

Hemidactylium scutatum (Caudata: Plethodontidae) is a small, four-toed salamander distributed throughout eastern North America. Characteristic of the family Plethodontidae, members of the genus *Hemidactylium* lack lungs and possess nasolabial grooves. As the sole species of the genus *Hemidactylium* and the monotypic tribe Hemidactyliini (one of four tribes of the subfamily Hemidactyliinae), *H. scutatum* possesses four digits on each hindlimb, mode V tongue feeding, and skulls with fully articulated frontal and parietal bones and no fontanelle (Wake, 2012). Adults inhabit terrestrial, forested habitats with access to fishless ponds that serve as breeding locations to support a biphasic life mode. Adults are easy to identify due to a constriction at the base of the tail and a white venter with a distinct black spot pattern. *H. scutatum* exhibits a short-lived, aquatic larval stage, which contrasts to the direct development mode utilized by most members of the family Plethodontidae. Adult females lay eggs during the late spring in nests of densely packed sphagnum moss patches alongside the edge of fresh water ponds. Egg clutches develop in the terrestrial nests until the gilled, aquatic larvae hatch and enter the pond for a short larval period resulting in metamorphosed juveniles that return to terrestrial habitats during the summer.

Broader understanding of embryonic morphological features and developmental patterns in *H. scutatum* may help resolve hypotheses regarding species diversity and the complex

* Corresponding author. James Madison University, USA. Tel.: +540 568 4830; fax: +540 568 4990.
E-mail address: hurneyca@jmu.edu (C.A. Hurney).
http://dx.doi.org/10.1016/j.mod.2014.12.007
0925-4773/

phylogenetic history of metamorphosis within the family Plethodontidae (Bonett et al., 2005; Bruce, 2005; Chippindale and Wiens, 2005; Kerney et al., 2012). Short-lived, long-lived, and direct developing species are contained within the subfamily Hemidactyliinae. Recent phylogenetic analyses indicate that the monotypic tribe Hemidactyliini is the sister taxon to the species-rich, direct-developing tribes Bolitoglossini and Batrachosepini (Vieites et al., 2011; Wake, 2012). Relations with members of the tribe Spelerpini, whose members exhibit long-lived larval stages as well as aquatic paedomorphs, remain poorly resolved.

Despite the call for more studies on salamander embryonic development, resolution of the debates regarding the phylogenetic history of Plethodontidae is limited by the lack of comprehensive descriptions of embryonic morphogenesis (Bonett et al., 2005; Bruce, 2005; Chippindale and Wiens, 2005). Most of the early reports of embryonic development in plethodontids are incomplete analyses based on field description or informal laboratory observations (Barden and Kezer, 1944; Bishop, 1920, 1925, 1941; Bishop and Chrisp, 1933; Fowler, 1946; Franz, 1967; Goin, 1951; Goodale, 1911; Hilton, 1909; Humphrey, 1928; Lynn and Dent, 1941; Miller, 1944; Rabb, 1956; Smith et al., 1968; Stebbins, 1949). More recent staging tables offer more insights into embryonic features, but many are not comprehensive or do not document the full embryonic period (Collazo and Keller, 2010; Collazo and Marks, 1994; Franssen et al., 2005; Marks, 1995; Marks and Collazo, 1998). The embryonic staging table for the direct-developing *Plethodon cinereus* provides the most comprehensive analysis of plethodontid embryonic characters to date (Kerney, 2011). The staging table of embryonic development for *H. scutatum* complements and extends previous studies and provides a complete analysis of timing and characterization of external development to extend knowledge of salamander embryology, vertebrate development, and further enrich analyses of plethodontid life history evolution.

2. Results

We define 28 embryonic stages for *H. scutatum* on the basis of external morphology. The total embryonic period from oviposition to hatching is approximately 45 days at 15 °C. Stages 1 to 19 represent early development from cleavage through neurulation and are consistent with stage designations for events through neurulation defined for *Ambystoma mexicanum* (Bordzilovskaya et al., 1989), *Ambystoma maculatum* (Harrison, 1969), *Desmognathus aeneus* (Marks and Collazo, 1998), and *Xenopus laevis* (Nieuwkoop and Faber, 1956). Stages 20 through 28 document later developmental events such as tail, gill, and limb formation culminating in hatching (Stage 28). After neurulation, *H. scutatum* development deviates from described amphibian species and thus we define stages 20–28 based solely on the appearance and change in external morphology. Landmark features of each stage are summarized (Tables 1–3) and illustrations of each stage are presented (Figs. 1–6), where each illustration (or set of illustrations) depicts diagnostic external features that characterize a unique stage ofembryonic development.

2.1. *Major features of early development: stages 1–19 (Tables 1 and 2; Figs. 1, 2, 3 and 4)*

2.1.1. *Cleavage stages (Stages 1–7; 0–27 hours after oviposition; Table 1; Fig. 1)*

H. scutatum embryos have lightly pigmented animal poles and no evidence of gray crescent pigmentation on the dorsolateral edge. Single-celled embryos average 2.4 mm in diameter (n = 7; range 2.3 mm–2.5 mm (Stage 1), which is consistent with previous reports from Humphrey (1928) and Bishop (1920). As observed in most amphibians, cleavage in *H. scutatum* embryos is asymmetrical and holoblastic. The first and second cleavage planes in *H. scutatum* are meridional and orthogonal to one another. The first cleavage plane begins to form approximately 8 hours after oviposition and division is complete within 12 hours (Stage 2). Before the first cleavage furrow is complete, a second furrow begins to form in the animal pole. The first two cleavages divide the embryo into four cells by the end of Stage 3 (15 h). The third cleavage event is equatorial and displaced toward the animal pole creating 4 micromeres in the animal hemisphere and 4 macromeres in the vegetal hemisphere observable externally (Stage 4, 18 h). After the 8-cell stage, cell division continues asymmetrically and synchronously, resulting in an increase of cell number from 16 cells (Stage 5, 21 h) to 32 cells (Stage 6, 24 h) and ultimately to 64 cells (Stage 7, 27 h). Time-lapse movies at room temperature (22–23 °C) show that the interval between the onset of early cleavages decreases throughout development. For example, 2 hours and 40 minutes elapse between second and third cleavage, 2 hours and 10 minutes elapse between the third and fourth cleavage and 1 hour and 40 minutes elapse between sixth and seventh cleavage. Shorter intervals (1:35 or 1:30) occur for later cleavages. Thus developmental rates at room temperature are initially only moderately faster than at 15 °C but tend toward twice as fast as the embryo progresses through cleavage stages. The overall size of the embryo increases slightly during cleavage stages from 2.4 mm in diameter to 2.5 mm (n = 4). Similar asymmetric cleavage patterns are reported for other plethodontids (Collazo, 1990; Collazo and Marks, 1994; Hilton, 1909; Kerney, 2011; Marks, 1995; Marks and Collazo, 1998), although field studies of two direct developing plethodontids, *Aneides lugubris* and *Batrachoseps wrighti*, report meroblastic cleavage for early cleavage stages, followed by holoblastic cleavage during later cleavage stages (Miller, 1944; Stebbins, 1949).

2.1.2. *Blastula stages (Stages 8–9; 1 d 16 h to 3 d 5 h after oviposition; Table 1; Fig. 1)*

H. scutatum embryos enter Stage 8 approximately 40 hours after oviposition when the size of the apical aspect of the animal blastomeres decreases by a factor of 2 relative to the previous stage. Asymmetric cell division continues, resulting in hundreds of animal blastomeres that remain smaller in size and greater in number than vegetal blastomeres. The next transition occurs approximately 2 days and 9 hours after oviposition when the animal hemisphere becomes smooth and lighter in color (Stage 9). Manual bisection of Stage 8 and 9 *H. scutatum* embryos confirmed the presence of a blastocoel roof two cell layers thick (data not shown). Embryos of the larval developing plethodontid, *Eurycea bislineata*, have 2 cell layers (Goodale,

Table 1 – Descriptions of embryonic Stages 1–16 of *Hemidactylium scutatum*.

Stage	Approx. time since oviposition	Description
1	0 hours	One cell; the animal pole is heavily pigmented compared to the vegetal pole. The presence of the germinal vesicle is evident by an area of lighter pigmentation in the animal pole. The first cleavage furrow begins to form in the animal pole after 8 hours.
2	12 hours	Two cells; the cleavage furrow expands meridionally through the animal pole to divide the embryo into two equal cells. The cleavage plane is not complete in the vegetal pole as the second furrow begins to form.
3	15 hours	Four cells; a second meridional cleavage plane occurs perpendicular to the first and expands through the animal pole. Four blastomeres form when both divisions are complete.
4	18 hours	Eight cells; the third cleavage is equatorial and displaced toward the animal pole, creating asymmetry with four micromeres in the animal pole and four macromeres in the vegetal pole
5	21 hours	Sixteen cells; cell division continues synchronously, but asymmetrically in the animal and vegetal poles, creating 16 blastomeres. The animal pole remains darker than the vegetal pole.
6	24 hours	Thirty-two cells; cell division continues asymmetrically, creating animal blastomeres that are approximately 1/2 the size of those in Stage 5.
7	27 hours	Sixty-four cells; cell division continues asymmetrically, forming animal blastomeres that are approximately 1/2 the size of those in Stage 6.
8	1 day 16 hours	Early blastula; cell division becomes asynchronous and continues asymmetrically to form animal blastomeres that are approximately 1/2 the size of those in Stage 7.
9	2days 9 hours	Late blastula; cell division continues and the surface of the animal cap is smooth. Cells are too numerous to plausibly count and are individually pigmented. The animal pole is lighter than previous stages.
10	3 days 6 hours	Early gastrula; the first external sign of gastrulation appears as a dark blastopore lip on the dorsovegetal surface of the embryo. The animal pole often appears wrinkled.
11	4 days	Mid gastrula; as gastrulation continues, the blastopore lip elongates and becomes crescent shaped with the ends pointing ventrolaterally away from the future dorsal surface of the embryo. Involuting suprablastoporal cells are distinctly smaller than sub-blastoporal cells moving under the vegetal side of the blastopore lip.
12	5 days	Late gastrula; blastopore lip shortens to form a deep horizontal slit that is darkly pigmented at the ends.
13	7 days	Early neural plate; the blastopore lip elongates and becomes crescent shaped with the ends pointing anteriorly. The neural plate is slightly elevated from the dorsal surface and a shallow neural groove is present on anterior end of neural plate. The neural folds are not yet visible.
14	7 days 6 hours	Mid neural plate; the neural folds begin to emerge and elevate as the neural groove continues to deepen along the anterior end of the plate. The blastopore lip flattens and decreases in length.
15	8 days	Late neural plate; the neural folds continue to elevate and approach each other to form an "hourglass" shape. The neural groove is present along the length of the plate.
16	8 days 3 hours	Early neural fusion; the neural folds continue to elevate and approach with initial contact occurring near the midbrain/hindbrain boundary of the forming neural tube. The blastopore is enclosed by the posterior end of the neural folds.

1911), while embryos of the larval developing *Desmognathus fuscus* have blastocoel roofs with only one cell layer (Hilton, 1911). *Ensatina eschscholtzii*, a direct developing plethodontid, also has embryos with one cell layer over the blastocoel (Collazo and Keller, 2010).

2.1.3. Gastrula stages (Stages 10–13; 3 d 6 h to 7 d after oviposition; Table 1; Fig. 2)

The first sign of gastrulation is evident approximately 3 days and 6 hours after oviposition when the blastopore lip appears as a dark invagination on the dorso-vegetal side of embryos of *H. scutatum* (Stage 10). Time lapse movies show that a large area of both dorsal marginal zone and dorsal vegetal endodermal tissue apically contract to form the initial blastopore lip, about 40–60 degrees in animal vegetal extent and 70–80 degrees in medio-lateral extent, forming a structure that is only a few degrees in animal vegetal extent, and about 30–45 degrees in medio-lateral extent. Endoderm around the vegetal pole also undergoes a great deal of contraction prior to and during dorsal blastopore lip formation. As gastrulation proceeds, marginal zone tissue involutes around the dorsal and lateral blastopore lip while large amounts of tissue moves through the vegetal side of the blastopore. Unlike *Ambystoma* (Shook et al., 2002), there is no involution of ventral marginal zone tissue around a blastopore. As involution continues, the blastopore lip undergoes multiple shape changes that define Stages 11, 12, and 13 (4 d, 5 d, and 7 d, respectively; estimates from movies at room temperature are 17 hours from Stages 11 to 12 and 20 hours from Stages 12 to 13). The blastopore lip elongates to form a roughly third-circle crescent with ends that point laterally (Stage 11) that grows to a half-circle crescent which persists 10 or 12 hours at room temperature, but keeps getting smaller. Rather than completing the blastopore ventrally, the lip eventually shortens to form a horizontal slit with darkly pigmented ends (Stage 12). The blastopore lip increases in length again with ends that curve dorsally, around the posterior end of the early neural plate (Stage 13). Movement of ventral tissue under the blastopore lip and involution around the dorsal lip ends at or shortly after the transition from ventral-pointing to dorsal pointing blastopore lip. Thus the flat blastopore lip

Table 2 – Descriptions of embryonic Stages 17–21 of *Hemidactylium scutatum*.

Stage	Approx. time since oviposition	Description
17	9 days	Late neural fusion; the anterior folds are fused and the prospective brain regions are apparent. The folds continue to fuse posteriorly to form a "keyhole" shaped neural plate.
18	9 days 3 hours	Early neural tube; the neural folds are fused along the entire length of the embryo to form a suture. Further extension and development of the cranial regions of the neural tube are apparent. A head fold begins to become apparent.
19	10 days	Late neural tube; suture of neural tube is smooth along the length of the embryo. Neural development continues to progress as the most anterior regions of the developing brain continue to enlarge and the neural tissue as a whole extends. The head fold is more apparent and continues to separate the head from the ventral portion of the embryo.
20	11 days	The branchial plate is divided into two mounds, the largest and most posterior is the gill mound. During this stage, the branchial plate divisions become more evident with the development of grooves between each arch. The blastopore is a small slit anterior to the tail bud. Anteriorly, the optic vesicles are prominent lateral to the closed neural tube and the head is undercut to the first branchial mound. The tail bud is evident as a swelling at the posterior end of the embryo.
21	14 days	The forelimb bud (posterior) and the gill mound (anterior) are more prominent and spherical. The head is further undercut to the gill arches. The divisions of the branchial plate are more evident as the pharyngeal grooves clearly divide the mandibular, hyoid, and gill arches. The mandibular arch is prominent laterally and moves toward the ventral midline. The optic cup shows faint dorsal and lateral pigmentation and the lens placode invaginates to form the lens pit. The tail bud is rounded and undercut from the embryo. The embryo has a visible heartbeat and shows a motor response to mechanical stimuli.

stage appears to mark the approximate end of gastrulation. Time-lapse movies show that the dorsal curvature of the blastopore is associated with the dorsal convergence of the neural plate and the ectodermal tissue lateral to it.

These observations are consistent with previous analysis of *H. scutatum* embryos (Humphrey, 1928) but differ a great deal from the pattern of blastopore closure observed in other anurans, like *X. laevis*, in that there is no significant ventral lip, and shows substantial differences with the type of blastopore closure in other urodeles, such as *Ambystoma*, because such a large amount of ventral tissue moves directly under the dorsal blastopore lip, rather than involuting around a ventral lip (Keller and Shook, 2004). In certain regards, gastrulation in *H. scutatum* resembles gastrulation in reptiles (Bertocchini et al., 2013), as well as more primitive chordate gastrulation, in that there is no ventral lip, which may be a primitive trait (discussed in Shook and Keller, 2008). A complete yolk plug is formed in most larval and direct developers of the subfamily Plethodontinae with the exception of *P. cinereus* (Collazo, 1990; Dent, 1941; Marks, 1995; Marks and Collazo, 1998). Among the Plethodontidae, only the embryos of the larval developer, *E. bislineata*, have little to no ventral blastopore and undergo similar changes in morphology as seen in *H. scutatum* during gastrulation (Goodale, 1911). In contrast, there are several exceptions to complete blastopore formation in other families of urodeles as seen in some members of the genus, *Ensatina*, and the gigantic salamander, *Megalobtrachus maximus* (Collazo and Keller, 2010; Ichikawa, 1905).

2.1.4. *Neurula stages (Stages 13–19; 7 d to 10 d after oviposition; Tables 1 and 2; Figs. 3 and 4)*

Approximately 7 days after oviposition the neural plate of *H. scutatum* embryos is slightly elevated with a shallow neural groove and, as described above, the blastopore lip increases in length and curves around the posterior end of the early neural plate (Stage 13). During the next 6 hours, the neural folds emerge as the neural groove continues to deepen along the length of the neural plate (Stage 14). As neurulation continues, the neural folds become more prominent and the blastopore lip flattens again and decreases its width as the posterior neural folds close over it. During Stage 15 (8 d) the neural folds begin to form an "hourglass" shape. Initial contact and fusion of neural folds occurs toward the anterior end, near the future midbrain/hindbrain boundary (Stage 16, 8 d 3 h). The neural folds fuse bi-directionally over the next 2 days: the anterior portion of the neural tube forms by day 9 (Stage 17) while fusion of the posterior region continues for another 3 hours, resulting in a completely sutured neural tube (Stage 18). Primary fusion of the neural folds in the anterior region of the neural plate is atypical of amphibians (Duellman and Trueb, 1986), though it has been reported in one newt, *Triturus pyrrhogaster* (Anderson, 1943) and in the plethodontid salamander, *E. bislineata* (Goodale, 1911). Neurulation is complete by day 10 when the suture of the neural tube is smooth (Stage 19). Cranial development begins during Stages 18 and 19 as the most anterior regions of the developing brain begin to enlarge and extend.

2.2. *Major features of late development: Stages 20–28 (Tables 2 and 3; Figs. 5, 6, and 7)*

2.2.1. *Yolk reduction*

The ventral side of the *H. scutatum* embryo still contains much of the yolk volume 11 days after oviposition (Stage 20). In contrast, direct developing salamanders such as *A. lugubris* and *P. cinereus* embryos develop upon a large ventral yolk mass (Kerney, 2011; Miller, 1944; Piersol, 1910) or have yolk enclosed in abdominal folds (Marks and Collazo, 1998). Interestingly, *Pseudotriton ruber*, a larval developer, also exhibits a large ventral yolk mass (Bishop, 1925). The amount of yolk

Table 3 – Descriptions of embryonic Stages 22–28 of *Hemidactylium scutatum*.

Stage	Approx. time since oviposition	Description
22	18 days	The optic cup pigmentation is crescent shaped and becomes torus shaped with the choroid fissure still open at the end of the stage. The nasal pits are invaginated. The gill arch is tripartite and divides into three rami by the end of the stage. The cardiac prominence is evident. The amount of yolk is reduced. The length of the tail is approximately twice its dorsal-ventral height.
23	22 days	The pigmentation of the optic cup forms a complete circle and the choroid fissure closes. The right and left mandibular arches meet in the ventral midline and fuse. The gular fold fuses in the ventral midline. The third gill rami elongate first; later in the stage, the second gill rami elongate to approximately the same length as the third gill rami. Melanophores, initially of greatest concentration at the dorsal branchial region, spread throughout the dorsal surface of the head and trunk to reach the gill rami, forelimbs, and base of the tail by the end of the stage. The tail flattens laterally. The dorsal fin extends anteriorly from the tip of the tail to the posterior half of the trunk. The ventral fin is evident from the cloaca to the tip of the tail.
24	25 days	Optic cup pigmentation intensifies. The third gill rami are the first to branch, followed by the second typically a day later. The median notch of the gular fold indents and the edges of the fold become more distinct, forming a flap. Melanophores increase in concentration along the length of the head, trunk and tail. Bilaterally staggered spots begin to form along the dorsum of the anterior trunk, suggestive of the future larval pigmentation pattern. At the beginning of the stage, the distal end of the forelimb is polygonal. The hindlimb bud is present anterior to the cloaca and has melanophores on its dorsum. The dorsal fin extends anteriorly, spanning nearly 3/4 the length of the trunk. Both the dorsal and ventral fins increase in height.
25	28 days	The ventral cranial tissues become translucent between the mandibular cartilage and the gular fold. All three gill rami are branched; the second and third rami are branched more than the first. The larval pigmentation pattern is evident as the melanophore concentration increases, xanthophores appear along the dorsum and forelimbs, and the dorsal spot pattern extends throughout the trunk and into the tail. A few melanophores appear on the pericardium. The forelimb axis begins to change shape as wrist and elbow joints differentiate. The second digit extends beyond the first and third digit buds. By the end of the stage, the distal end of the hindlimb bud is paddle shaped. The vitelline vein is prominent ventrally and lateral vascularization increases as the amount of yolk decreases.
26	33 days	The forelimb has three distinct digits. A dark horizontal stripe forms, passing through the eye and nasal pits along the lateral aspect of the head. Green-reflecting iridophores appear in the eye. The median notch of the gular fold further indents. Pericardial pigmentation increases. Toward the end of the stage, the most anterior section of the gut curves into s-shapes. Xanthophores have migrated to the tail and are diffusely scattered in the ventral and dorsal fins.
27	37 days	The gular fold is biconvex and deepens. Pericardial pigmentation intensifies laterally. The forelimb has four digits; the second digit is greatest in length, followed by the third, first, and fourth. The elbow joint can bend to 90 degrees. Curving continues in the anterior part of the gut. The hindlimb buds are polygon shape with digit buds indicating the future first, second, and third toes. The knee joint has begun to differentiate.
28	45 days	The eyes are laterally placed and lidless, and have gold-reflecting iridophores. A few dark yellow xanthophores are diffusely scattered on the head, gills, forelimbs, and spots along the dorsum. The gills are elongate and highly branched. The second and third digits of the forelimb are equal in length. The venter is translucent from the cranium to the tail. The gut forms shaped patterns along the entire length. The hindlimb has three distinct digits and occasionally the fourth digit bud has begun to extend.

in *H. scutatum* embryos decreases during the next two stages while lateral ventral blood vessels become prominent by Stage 22. A more prominent blood vessel appears along the ventral side of the embryo and the amount of yolk continues to decrease during Stages 25 to 27. At hatching, a small amount of yolk persists posterior to the curved gut (Fig. 5). Hatchlings of larval developers, *Gyrinophilus porphyriticus*, *E. bislineata* and *D. fuscus* also exhibit reduced yolk (Collazo, 1990, 1996; Goin, 1951).

2.2.2. *Tail elongation*

The tail bud forms as a swelling just dorsal to the small slit-shaped blastopore about 1 day after the completion of neurulation (Stage 20, 11 d). Elongation results in a bluntly rounded tail bud that extends posteriorly (Stage 21, 14 d). Approximately 4 days later the tail elongates to become twice as long as its dorso-ventral height (Stage 22, 18 d). The tail begins to flatten laterally and the tip becomes more pointed. The dorsal fin extends anteriorly from the tail tip to the posterior half of the trunk while the ventral fin extends from the tip toward the cloaca (Stage 23, 22 d). During Stage 24 (25 d) the dorsal fin extends further anteriorly to span nearly 3/4 the length of the trunk and the ventral fin extends to the posterior border of the cloaca. Both fins continue to increase in height as the tail lengthens (Stages 25 through 28). The resulting broad, keel-shaped tail is typical of pond-type larvae at hatching (Duellman and Trueb, 1986; Goin, 1951; Rabb, 1956), rather than stream dwellers (Petranka, 1998).

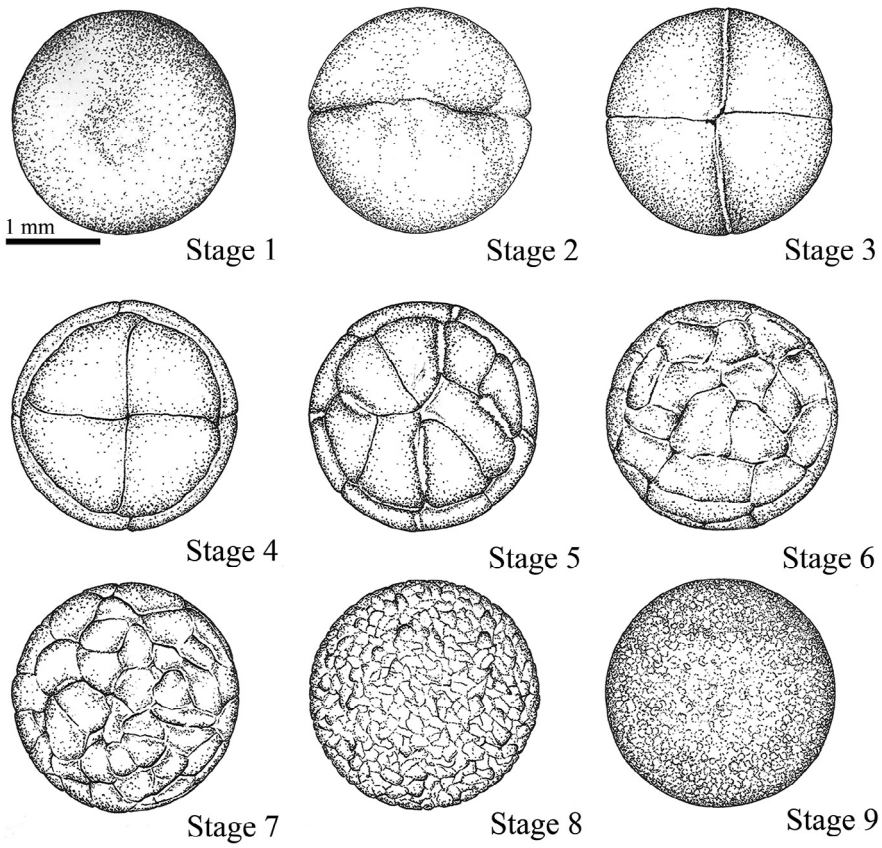

Fig. 1 – Sketches of cleavage Stages 1–9 of *Hemidactylium scutatum* highlighting dorsal views. 1 mm scale bar included for size reference.

2.2.3. *Eye development*

Optic vesicles are prominent in the developing head of *H. scutatum* embryos approximately 1 day after the completion of neurulation (Stage 20, 11 d). Faint pigmentation appears on the developing optic cup during the next 3 days and the lens placode invaginates to form the lens pit (Stage 21, 14 d). By the end of Stage 22 (18 d), optic cup pigmentation, which is initially crescent-shaped, intensifies around the edges to become torus-shaped with an open choroid fissure. The choroid fissure closes to produce optic pigmentation that fully encircles the lens pit (Stage 23, 22 d). Optic pigmentation continues to darken as the cornea forms (Stage 24, 25 d). Melanophores begin to form a dark horizontal stripe (Stage 26, 33 d) that becomes continuous across the lateral aspect of the head and snout by Stage 28 (45 d). Green and gold iridiophores appear concurrently with the formation of the horizontal stripe. Like other larval developers, *H. scutatum* hatchlings have laterally placed, lidless eyes (Bishop, 1925; Collazo and Marks, 1994; Marks, 1995), rather than the forward-oriented eyes of direct developers (Collazo, 1990; Dent, 1941; Kerney, 2011; Marks and Collazo, 1998).

2.2.4. *Gill development and branching*

The branchial plate is visible in *H. scutatum* embryos approximately 1 day after the completion of neurulation (Stage 20, 11 d). Pharyngeal grooves deepen during Stage 21 (14 d) and clearly delineate the gill arch from the mandibular and hyoid arches. The gill arch enlarges over the next 4 days and forms three gill rami (Stage 22, 18 d). The third gill ramus elongates during Stage 23 (22 d) followed by elongation of the second then first gill ramus. The third and second gill rami branch extensively during Stage 24 (25 d), while the first gill ramus branches during Stage 25 (28 d). Melanophores are present on all rami. Gill rami and branches continue to elongate until hatching. A similar sequence of gill rami formation, elongation, and branching occurs in *Desmognathus ochrophaeus, Desmognathus quadramaculatus, G. porphyriticus, P. cinereus, B. wrighti, A. lugubris,* and *E. eschscholtzii* (Collazo, 1990; Collazo and Marks, 1994; Dent, 1941; Marks, 1995; Marks and Collazo, 1998; Miller, 1944). In contrast, the second rami branch first during gill development in *D. aeneus*, while the first rami branch first in *Batrachoseps attenuatus* embryos (Collazo, 1990; Marks and Collazo, 1998). The extent of embryonic branching in the gills varies throughout the family Plethodontidae. Larval developers (*D. quadramaculatus, G. porphyriticus*) and direct developers (*D. aeneus*, and *P. cinereus*) have long rami that are highly branched similar to the rami described for *H. scutatum* (Collazo and Marks, 1994; Kerney, 2011; Marks and Collazo, 1998). *D. ochrophaeus, A. lugubris,* and *E. eschscholtzii* have short gills that do not branch or are not highly branched (Collazo, 1990; Marks, 1995; Miller, 1944).

At hatching, the pond-type larvae of *H. scutatum* have highly branched, long gills similar to *Eurycea quadridigitata* and *Stereochilus marginatus* (Petranka, 1998). Stream-type larvae typically have shorter gills that are not extensively branched, as

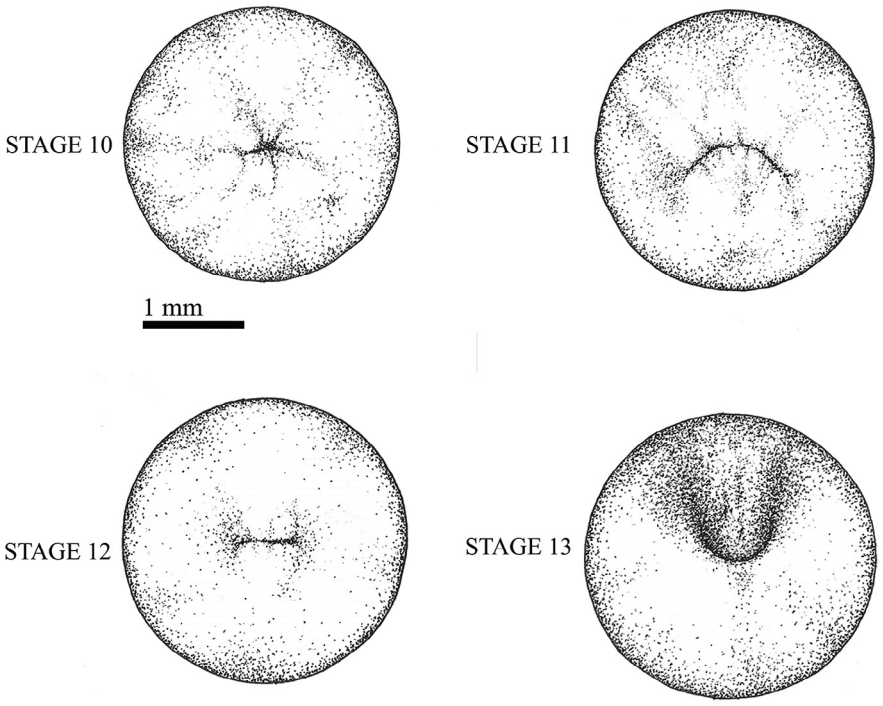

Fig. 2 – Sketches of gastrula Stages 10–13 of *Hemidactylium scutatum* highlighting dorsal views. 1 mm scale bar included for size reference.

reported for *G. porphyriticus*, *D. ochrophaeus*, and *P. ruber* (Bishop, 1925; Collazo and Marks, 1994; Marks, 1995). By contrast, the gills of direct developers (*B. wrighti*, *B. attenuatus*, *E. eschscholtzii*, *Bolitoglossa subpalmata*, *Bolitoglossa compacta*, *A. lugubris*, *P. cinereus*, and *D. aeneus*) are typically resorbed at the time of hatching or shortly thereafter (Collazo, 1990; Collazo and Marks, 1994; Dent, 1941; Hanken, 1979; Marks and Collazo, 1998; Miller, 1944; Stebbins, 1949).

2.2.5. *Limb formation*

The forelimb bud begins forming posterior to the branchial bud approximately 1 day after the completion of neurulation (Stage 20, 11 d) and is prominent by Stage 21 (14 d). Initially, the distal end of the forelimb bud is initially round (Stage 21, 14 d), then paddle-shaped, and ultimately polygonal in shape just prior to the appearance of digits (Stage 24, 25 d). The forelimb undergoes multiple changes during Stage

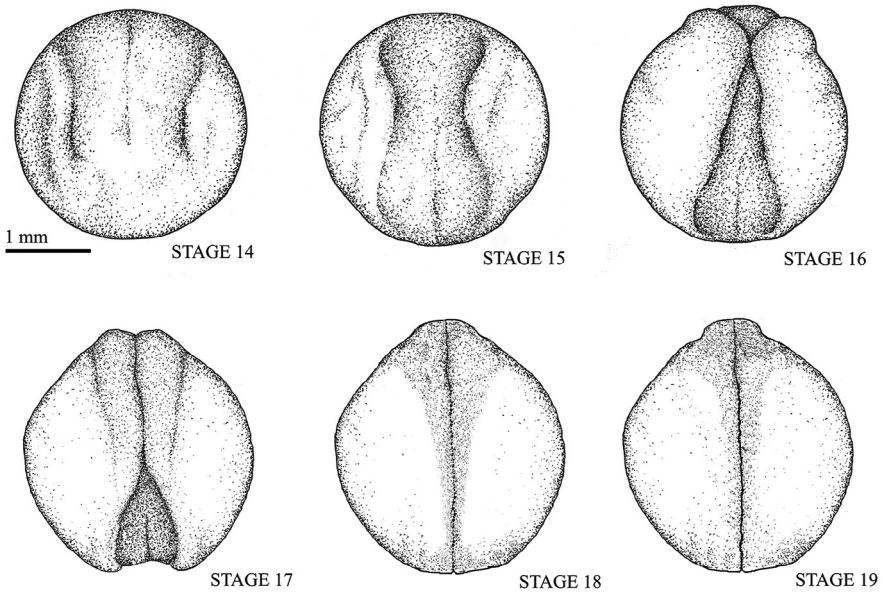

Fig. 3 – Sketches of neurula Stages 14–19 of *Hemidactylium scutatum* highlighting dorsal views. 1 mm scale bar included for size reference.

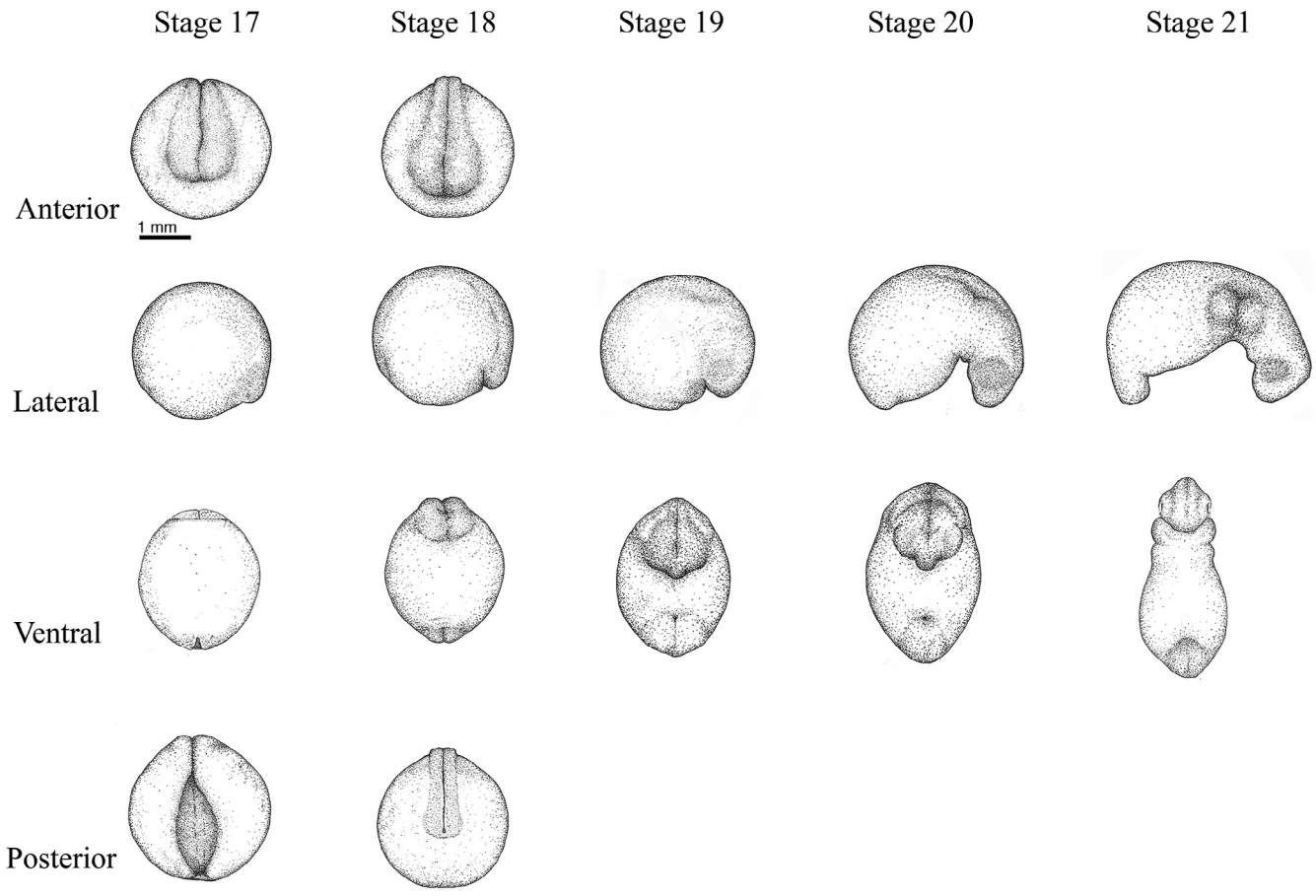

Fig. 4 – Sketches of embryonic Stages 17–21 of *Hemidactylium scutatum* highlighting select anterior, lateral, ventral and posterior views. 1 mm scale bar included for size reference.

25 (28 d), including the presence of melanophores and xanthophores on the dorsal surface, the differentiation of wrist and elbow joints, and the appearance of digits. At Stage 26 (33 d), digit 2 is notably greater in length than digit 3 and the newly forming digit 1. Four digits are present by Stage 27 (37 d) with the respective lengths being digit 2 > 3 > 1 > 4. Forelimbs are mobile and bend 90° at the elbow. As hatching approaches, the forelimb is well developed with the respective digit lengths, 2 = 3 > 1 > 4 (Stage 28, 45 d).

The hindlimb bud appears at Stage 24 (25 d; approximately 11 days after the appearance of the forelimb bud) with melanophores present on the dorsal surface. The distal end of the hindlimb bud is initially round and becomes paddle-shaped by the end of Stage

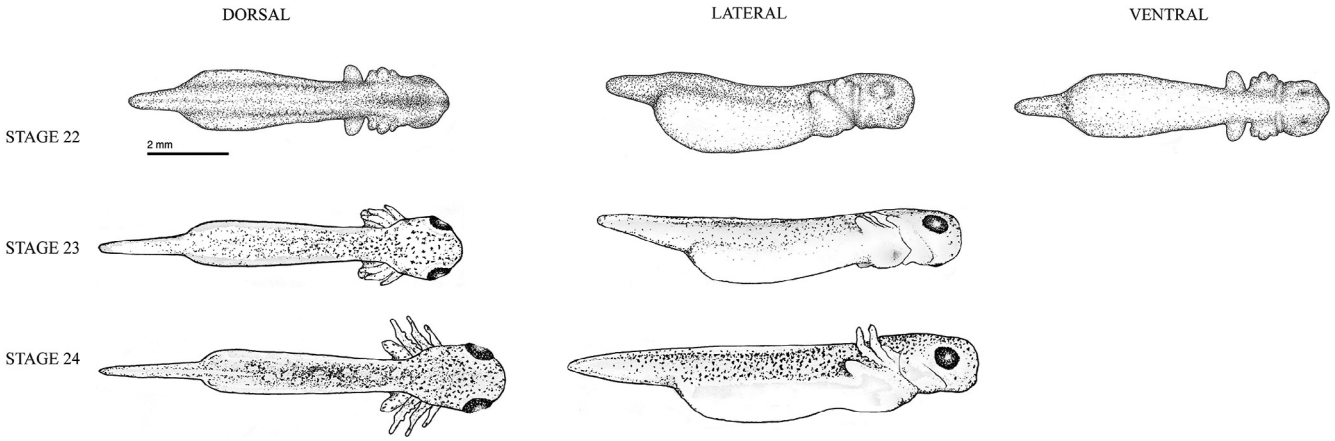

Fig. 5 – Sketches of embryonic Stages 22–24 of *Hemidactylium scutatum* highlighting select dorsal, lateral and ventral views. 2 mm scale bar included for size reference.

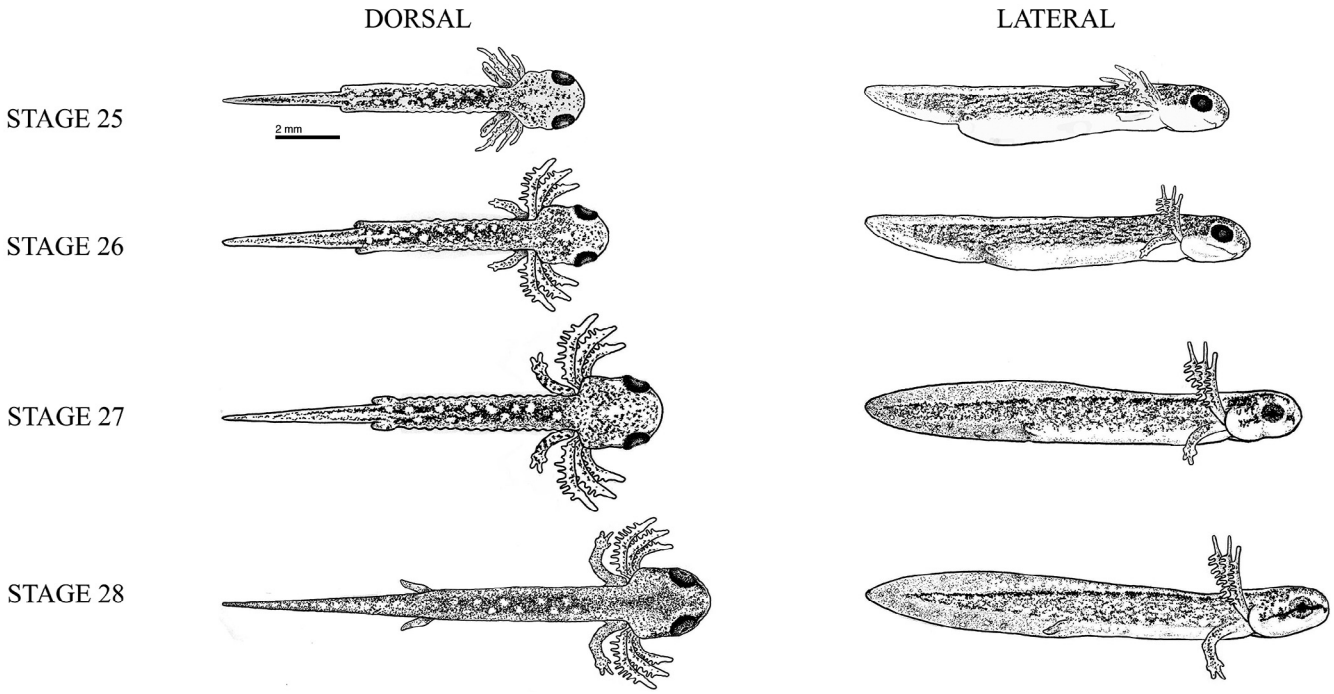

Fig. 6 – Sketches of embryonic Stages 25–28 of *Hemidactylium scutatum* highlighting select dorsal and lateral views. 2 mm scale bar included for size reference.

25 (28 d) and polygonal in shape just prior to the appearance of digits (Stage 27, 37 d). A differentiated knee and three digits, occasionally four, are present at hatching (Stage 28, 45 d).

Forelimbs typically develop before the hindlimbs in most of the described plethodontid larval developers, including *H. scutatum*, *G. porphyriticus*, *P. ruber*, *Desmognathus monticola*, and *E. bislineata* (Bishop, 1925; Collazo, 1990; Marks and Collazo, 1998) and one direct developer, *B. subpalmata*. Direct developers and some larval developers have almost synchronous appearance and development of the forelimbs and hindlimbs, as reported in *D. aeneus*, *D. quadramaculatus*, *D. ochrophaeus*, *E. eschscholtzii*, and *B. attenuatus* (Collazo, 1990; Marks, 1995; Marks and Collazo, 1998). The adult complement of forelimb digits is well formed at the time of hatching in *H. scutatum*, while the hindlimbs rarely display fully developed digits. Similar patterns have been reported for the larval developer *G. porphyriticus* (Collazo and Marks, 1994). Direct developers (*P. cinereus*, *D. aeneus*)

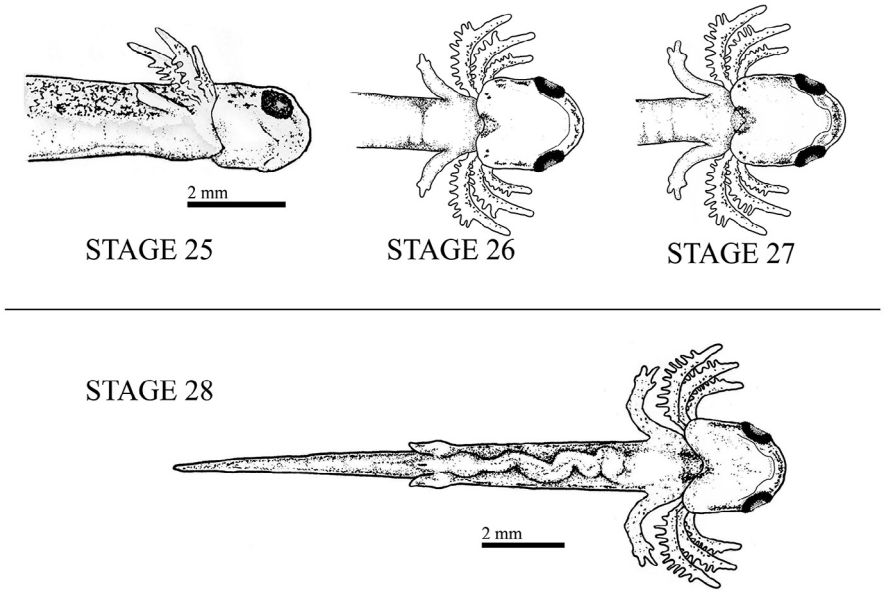

Fig. 7 – Sketches of embryonic Stages 25–28 of *Hemidactylium scutatum* highlighting select ventral and lateral views. 2 mm scale bar included for size reference.

and some larval developers (*A. lugubris, D. fuscus*) have the adult complement of digits on both forelimbs and hindlimbs at hatching (Dent, 1941; Goin, 1951; Hilton, 1909; Marks and Collazo, 1998; Miller, 1944; Piersol, 1910).

2.2.6. *Pigmentation changes*

Melanophores first appear dorsal to the branchial region and migrate throughout the dorsal surface of the head and trunk to reach the gill rami, forelimbs, and base of tail (Stage 23, 22 d). The yolk gives a yellowish color to the venter. Melanophore pigmentation intensifies along the dorso-lateral length of the embryo and a series of staggered bilateral spots (absence of melanophores) appear on the anterior dorsum of the trunk (Stage 24, 25 d). A few days later the dorsal spot pattern extends throughout the trunk and tail while xanthophores appear along the dorsum and forelimbs; anterior ventral tissues become translucent between the mandible and gular fold (Stage 25, 28 d). Melanophores appear in the pericardium (Stage 25) and pigmentation intensifies during Stages 26 and 27 (33–37 d). Xanthophores migrate into the tail and are diffusely scattered in dorsal and ventral fins (Stage 26, 33 d). As the yolk reduces, the heart, blood vessels, stomach, and other organs can be seen through the skin (Stages 26 to 28). A few dark yellow xanthophores are present on the head, gills, forelimbs, trunk and tail (Stage 28, 45 d). The larval pigmentation pattern is established by hatching (Stage 28, 45) and consists of 6 to 8 pairs of staggered yellowish spots on a mottled dark dorsum with a translucent venter and darkly pigmented pericardium.

Development of the species-specific larval pigmentation pattern in *H. scutatum* is similar to the process observed in embryos of larval developing plethodontids, including *G. porphyriticus*, *Eurycea longicauda*, *Eurycea lucifuga*, *E. quadridigitata*, *Desmognathus auriculatus*, *D. quadramaculatus, D. ochrophaeus,* and *P. ruber* (Bishop, 1925; Collazo and Marks, 1994; Franz, 1967; Goin, 1951; Hutchison, 1958; Marks, 1995). In contrast, hatchlings of direct developers (*P. cinereus*, *B. attenuatus, E. eschscholtzii*, *D. aeneus*, and *B. wrighti*) display pigmentation patterns that reflect the adult pigmentation (Collazo, 1990; Dent, 1941; Marks and Collazo, 1998; Piersol, 1910; Stebbins, 1949).

3. Experimental procedures

3.1. *Collection and maintenance of* Hemidactylium scutatum *embryos*

Portions of terrestrial egg clutches (n = 13) from naturally ovipositing females were collected from the George Washington National Forest in Rockingham (2002, 2004) and Botetourt (2005, 2006) counties of Virginia. One naturally ovipositing female from Rockingham County was maintained on moistened filter paper and moss in the lab for less than one week (2004). Field collected embryos ranged from day 1 to day 18 of the estimated 45-day embryonic period. Jelly coats and egg membranes were removed from some embryos manually using fine forceps; representative clutch-mates were intact until hatching. All embryos were maintained at 15 °C on moistened filter paper; those without membranes were submerged in artificial pond water (Wyngaard and Chinnappa, 1982). All images were collected at room temperature and specimens were returned to 15 °C immediately.

3.2. *Monitoring embryonic development*

Observations and photographs of 32 individual, unanesthetized embryos were taken at intervals of 12 or 24 hour using a Leica Wild M8 microscope with a Hamamatsu CCD camera (2002, 2004, 2005) or a Zeiss Stemi SV6 microscope with an Insight camera (2006). Photographs of clutch-mates were taken at less frequent intervals. Images were time-stamped such that intervals between observable changes in morphology were documented. All linear and area measurements were collected from images cited above using Oncor 1.7 (2002, 2004, 2005) and Spot v.4 (2006) image analysis software. Representative image sets for each stage can be found in the Dryad Digital Repository.

Time-lapse sequences (1 frame every 5 minutes) during cleavage, gastrulation, and neurulation were compiled from about 50 embryos maintained at 21–23 °C. Images were captured using a Zeiss SV6 microscope with a Dage MTI CCD-72 camera via NIH image 1.6 or Scion image capture software or using an Olympus IX70 inverted microscope with a Hamamatsu CCD-4742 camera via Metamorph software. Representative movies can be found in the Dryad Digital Repository.

Six embryos were fixed in Smith's fixative, placed in 6% agarose gel, and bisected to confirm the presence of a blastocoel. The surfaces of two embryos were stained with a crystallized piece of Nile Blue using fine forceps to establish the pattern of neural tube fusion.

3.3. *Preparation of developmental series*

Total developmental time for *H. scutatum* (reared at 15 °C) was estimated by combining data from multiple embryos from several clutches with overlapping developmental stages. We were able to confirm time of oviposition for one embryo oviposited by an adult female maintained in the lab. Thirteen of the 32 individuals photographed at regular intervals were documented for 30 or more consecutive days; individuals undergoing key changes in morphology were photographed more frequently. Clutch mates of multiple individuals were maintained in jelly coats and egg membranes and reared to natural hatching.

Our goal in dividing the embryonic period of *H. scutatum* into discrete developmental stages was to facilitate meaningful comparison with existing amphibian staging tables and to generate a useful tool for experimentation in which each stage reflects readily observable changes in external morphology. Thus, each stage represents a period of time during which diagnostic features undergo prominent changes. Hand-drawn illustrations highlight stage-specific features and were generated to scale using multiple images. Principal diagnostic features are those typical of amphibian staging tables (Bordzilovskaya et al., 1989; Harrison, 1969; Marks and Collazo, 1998; Nieuwkoop and Faber, 1956) and include cell number, formation of a blastocoel, shape of blastopore, formation of the neural tube, yolk reduction, and aspects of the development of the tail, eyes, gills, limbs, and pigmentation.

4. Discussion

This study provides the first comprehensive description of the embryonic development of the plethodontid salamander, *Hemidactylium scutatum*. Embryos of the four-toed salamander develop into free-swimming larvae over a 45-day period represented by 28 distinct stages. With regard to early embryonic development (Stages 1–19), our results confirm previous work on *H. scutatum* (Bishop, 1920; Humphrey, 1928) yet are detailed enough to facilitate comparisons with amphibian model organisms (e.g. *Xenopus* and *Ambystoma*) in terms of timing, sequence, and pattern variations. Later developmental stages (Stages 20–28) reveal diagnostic features that may prove useful for additional research related to the life history evolution in the family Plethodontidae and comparative embryological studies with other salamanders.

Embryos of *H. scutatum* exhibit asymmetric, holoblastic cleavage pattern resulting in a blastula with a two-cell layer thick blastocoel roof. Gastrulation commences with the formation of a blastopore lip that undergoes numerous shape changes while marginal zone and vegetal tissue involutes and moves through the blastopore. The neural plate forms an hour-glass shape with primary fusion of the neural folds occurring in the anterior region of the embryo and closes bi-directionally forming the neural tube. *H. scutatum* embryos are yolk-rich and retain a large ventral yolk mass until the gut begins to form near the end of the embryonic period.

Analysis of the timing of later developmental events reveals that tail, eye, gill, and forelimb development begin around day 11 (Stage 20) with the formation of the tailbud, optic vesicles, branchial plates and forelimb buds. As the development of these structures continues, pigmentation appears on various embryonic structures, including the dorsal side of the embryo, eyes, gills, forelimbs, and tail around day 22 (Stage 23). Hindlimb buds appear on day 25 (Stage 24) and digit formation begins just prior to hatching on day 45. Upon hatching, *H. scutatum* larvae have broad, keel shaped tails that continue to segment and elongate during morphogenesis through adulthood (Babcock and Blais, 2001; Vaglia et al., 1997). The highly pigmented larvae have laterally placed, lidless eyes and display tripartite gills with extensive branching and blood supply. Larval forelimbs display 4 digits along with wrist and elbow joints, while hindlimbs display only 3 digits, occasionally 4.

Current knowledge of vertebrate development is predominantly based on studies of a few well-known, lab-reared species (Gilbert, 2005; Wilt and Hake, 2004; Wolpert, 2002). Generalization of developmental patterns based on a few vertebrate model systems limits our conclusions about developmental mechanisms and homologies of developmental processes (Bolker, 1995; Marks and Collazo, 1998; Richardson et al., 1997; Wake, 2003). Classical descriptive embryology of more diverse species and developmental modes is fundamentally important to increasing our understanding of developmental processes and mechanisms. Understanding the more complex mechanisms of larval and direct development requires an increase in descriptive developmental studies (Wake and Hanken, 1996) and creative approaches to overcoming obstacles for studying plethodontid embryos, such as embryo availability (Bruce, 2005; Wake and Hanken, 1996).

For over a century developmental biologists have been documenting stages of amphibian embryonic development. Seminal contributions include the normal table of development of *Xenoups laevis* by Nieuwkoop and Faber (1956) and contributions on the development of *Ambystoma maculatum* embryos (Harrison, 1969) and *Ambystoma mexicanum* (Bordzilovskaya et al., 1989). Although not often viewed as results, these tools represent some of the most cited papers in developmental biology (Hopwood, 2007). More importantly, these tools provide a foundation for research into complex developmental phenomena, plasticity in life history evolution, and phylogenetic analyses. Further studies of this nature will aid interspecific comparisons within and outside the family Plethodontidae and may reveal underlying developmental patterns or features among larval and direct developers.

Acknowledgements

We want to acknowledge the undergraduate and graduate students who worked tirelessly on this project. We are grateful to our colleagues who supported this research by providing a stimulating academic work environment. Funding for this research came from a grant from the Jeffress Memorial Trust (J-807) to Carol Hurney, and a NIH merit award (R37HD025594) to Ray Keller (P.I.) and David Shook.

REFERENCES

Anderson, P.L., 1943. The normal development of *Triturus pyrrhogaster*. Anat. Record. 86, 59–73.

Babcock, S.K., Blais, J.L., 2001. Caudal vertebral development and morphology in three salamanders with complex life cycles (*Ambystoma jeffersonianum*, *Hemidactylium scutatum*, and *Desmognathus ocoee*). J. Morphol. 247 (2), 142–159.

Barden, R.B., Kezer, L.J., 1944. The eggs of certain plethodontid salamanders obtained by pituitary gland implantation. Copeia 1944, 115–118.

Bertocchini, F., Alev, C.Y., Nakaya, Y., Sheng, G., 2013. A little winning streak: the reptilian-eye view of gastrulation in birds. Develop. Growth Differ. 55, 52–59.

Bishop, S.C., 1920. Notes on the habits and development of the four-toed salamander, *Hemidactylium scutatum* (Schlegel). Bull. New York State Mus. 219, 251–282.

Bishop, S.C., 1925. The life of the Red Salamander. Nat. Hist. 25, 385–389.

Bishop, S.C., 1941. The salamanders of New York. Bull. New York State Mus. 324, 1–365.

Bishop, S.C., Chrisp, H.P., 1933. The nests and young of the Allegheny Salamander *Desmognathus fuscus ochrophaeus*. Copeia 1933, 194–198.

Bolker, J.A., 1995. Model systems in developmental biology. Bioessays 17, 451–455.

Bonett, R.M., Mueller, R.L., Wake, D.M., 2005. Why should reacquisition of larval stages by Desmognathine salamanders surprise us? Herp. Rev. 36, 112–113.

Bordzilovskaya, N.P., Dettlaff, T.A., Duhon, S.T., Malacinski, G.M., 1989. Developmental-stage series of axolotl embryos. In: Malacinski, A.J. (Ed.), Developmental Biology of the Axolotl. Oxford U Press, New York, pp. 201–219.

Bruce, R.C., 2005. Did *Desmognathus* salamanders reinvent the larval stage? Herp. Rev. 36, 107–112.

Chippindale, P.T., Wiens, J.J., 2005. Re-evolution of the larval stage in the plethodontid salamander genus *Desmognathus*. Herp. Rev. 36, 113–117.
Collazo, A. 1990. Development and evolution in the salamander family Plethodontidae. PhD Dissertation. University of California Berkeley.
Collazo, A., 1996. Evolutionary correlations between early development and life history in plethodontid salamanders and teleost fishes. Amer. Zool. 36, 116–131.
Collazo, A., Keller, R., 2010. Early development of *Ensatina eschscholtzii* an amphibian with a large, yolky egg. EvoDevo 1, 6.
Collazo, A., Marks, S.B., 1994. Development of *Gyrinophilus porphyriticus*: identification of the ancestral developmental pattern in the salamander family Plethdontidae. J. Exp. Zool. 268, 239–258.
Dent, J.N., 1941. The embryonic development of *Plethodon cinereus* as correlated with the differentiation and functioning of the thyroid gland. J. Morphol. 71, 577–601.
Duellman, W.E., Trueb, L., 1986. Biology of Amphibians. Johns Hopkins Press, Baltimore.
Fowler, J.A., 1946. The eggs of *Pseudotriton montanus montanus*. Herp. Notes 2, 105.
Franssen, R.A., Marks, S., Wake, D., Shubin, N., 2005. Limb chondrogenesis of the seepage salamander, *Desmognathus aeneus* (Amphibia:Plethodontidae). J. Morphol. 265, 87–101.
Franz, L.R., Jr., 1967. Notes on the long-tailed salamander, *Eurycea longicauda longicauda*, in Maryland caves. Bull. Md. Herpetol. Soc. 3, 1–6.
Gilbert, S.F., 2005. Developmental Biology, seventh ed. Sinauer Associates, Sunderland, MA.
Goin, C.J., 1951. Notes on the eggs and early larvae of three more Florida salamanders. Ann. Carnegie Mus. 32, 253–263.
Goodale, H.D., 1911. The early development of *Spelerpes bilineatus* (Green). Am. J. Anat. 12, 173–247.
Hanken, J., 1979. Egg development time and clutch size in two neotropical salamanders. Copeia 1979, 741–744.
Harrison, R.G., 1969. Harrison stages and description of the normal development of the Spotted Salamander, *Amblystoma punctatum* (Linn). In: Organization and Development of the Embryo. Yale University Press, New Haven, CT, pp. 44–66.
Hilton, W.A., 1909. General features of the early development of *Desmognathus fusca*. J. Morphol. 20, 533–547.
Hilton, W.A., 1911. Some remarks on the gastrulation of *Desmognathus fusca*. Biol. Bull. 21, 1–8.
Hopwood, N., 2007. A history of normal plates, tables and stages in vertebrate embryology. Int. J. Dev. Biol. 51, 1–26.
Humphrey, R.R., 1928. Ovulation in the Four-Toed salamander, *Hemidactylium scutatum*, and the external features of cleavage and gastrulation. Biol. Bull. 54, 307–323.
Hutchison, V.H., 1958. The distribution and ecology of *Eurycea lucifuga*. Ecol. Monogr. 28, 1–20.
Ichikawa, C., 1905. The gastrulation of the gigantic salamander, *Megalobatrachus maximus*. Zool. Mag. Tokyo Zool. Soc. 17, 26–28.
Keller, R., Shook, D., 2004. Gastrulation in amphibians. In: Stern, C.D. (Ed.), Gastrulation from Cells to Embryos. Cold Spring Harbor Laboratory Press, Cold Spring Harbor, NY, pp. 171–203.
Kerney, R., 2011. Embryonic staging table for a direct-developing salamander, *Plethodon cinereus* (Plethodontidae). Anat. Rec. 294, 1796–1808.
Kerney, R.R., Blackburn, D.C., Müller, H., Hanken, J., 2012. Do larval traits re-evolve? Evidence from the embryogenesis of a direct-developing salamander, *Plethodon cinereus*. Evolution 66, 252–262.
Lynn, W.G., Dent, J.N., 1941. Notes on *Plethodon cinereus* and *Hemidactylium scutatum* on Cape Cod. Copeia 1941, 113–114.
Marks, S.B. 1995. Development and evolution of the Dusky Salamanders (Genus *Desmognathus*). PhD Dissertation. University of California Berkeley.
Marks, S.B., Collazo, A., 1998. Direct development in *Desmognathus aeneus* (Caudata: Plethodontidae): a staging table. Copeia 1998, 637–648.
Miller, L., 1944. Notes on the eggs and larvae *Aneides lugubris*. Copeia 1944, 224–230.
Nieuwkoop, P.D., Faber, J., 1956. Normal Table of *Xenopus laevis laevis* (Daudin). Garland Publishing, North-Holland, Amsterdam.
Petranka, J.W., 1998. Salamanders of the United States and Canada. Smithsonian Institution Press, Washington, DC, pp. 290–295.
Piersol, W.H., 1910. The habits and larval state of *Plethodon cinereus erythronotus*. Trans. Can. Inst. 8, 469–493.
Rabb, G.B., 1956. Some observations on the salamander *Stereochilus marginatum*. Copeia 1956, 119.
Richardson, M.K., Hanken, J., Mayoni, L.G., Pieau, C., Raynaud, A., Selwood, L., et al., 1997. There is no highly conserved embryonic stage in the vertebrates: implications for current theories of evolution and development. Anat. Embryol. 196, 91–106.
Shook, D.R., Keller, R., 2008. Epithelial type, ingression, blastopore architecture and the evolution of chordate mesoderm morphogenesis. J. Exp. Zool. B Mol. Dev. Evol. 310, 85–110.
Shook, D.R., Majer, C., Keller, R., 2002. Urodeles remove mesoderm from the superficial layer by subduction through a bilateral primitive streak. Dev. Biol. 248, 220–239.
Smith, H.M., Landey, M.J., Underhill, D.K., 1968. Some characteristics of the eggs and embryos of a Mexican Plethodontid salamander. Herpetologica. 24, 67–72.
Stebbins, R.C., 1949. Observations on laying, development, and hatching of the eggs *Batrachoseps wrighti*. Copeia 1949, 161–168.
Vaglia, J.L., Babcock, S.K., Harris, R.N., 1997. Tail development and regeneration throughout the life cycle of the four-toed salamander *Hemidactylium scutatum*. J. Morphol. 233, 15–29.
Vieites, D.R., Nieto Román, S., Wake, M.H., Wake, D.B., 2011. A multigenic perspective on phylogenetic relationships in the largest family of salamander, the Plethodontidae. Mol. Phylogenet Evol. 59, 623–635.
Wake, D.B., 2012. Taxonomy of the Salamanders of the Family Plethodontidae (Amphibia: Caudata). Zootaxa 3484, 75–82.
Wake, D.B., Hanken, J., 1996. Direct development in the lungless salamanders: what are the consequences for developmental biology, evolution and phylogenesis? Int. J. Dev. Biol. 40, 859–869.
Wake, M.H., 2003. Reproductive modes, ontogenies, and the evolution of body form. Anim. Biol. 53, 209–223.
Wilt, F.H., Hake, S.C., 2004. Principles of Developmental Biology. WW Norton and Company Inc, New York.
Wolpert, L., 2002. Principles of Development, second ed. Oxford University Press, London.
Wyngaard, G.A., Chinnappa, C.C., 1982. General biology and cytology of cyclopoids. In: Developmental Biology of Freshwater Invertebrates. AR Liss, New York, pp. 485–533.